C–H Activation Hot Paper

How to cite: *Angew. Chem. Int. Ed.* **2022,** *61,* e202203624
International Edition: doi.org/10.1002/anie.202203624
German Edition: doi.org/10.1002/ange.202203624

Pd^{II}-Catalyzed C(alkenyl)–H Activation Facilitated by a Transient Directing Group**

Mingyu Liu, Juntao Sun, Tuğçe G. Erbay, Hui-Qi Ni, Raúl Martín-Montero, Peng Liu, and Keary M. Engle**

Abstract: Palladium(II)-catalyzed C(alkenyl)–H alkenylation enabled by a transient directing group (TDG) strategy is described. The dual catalytic process takes advantage of reversible condensation between an alkenyl aldehyde substrate and an amino acid TDG to facilitate coordination of the metal catalyst and subsequent C(alkenyl)–H activation by a tailored carboxylate base. The resulting palladacycle then engages an acceptor alkene, furnishing a 1,3-diene with high regio- and *E*/*Z*-selectivity. The reaction enables the synthesis of enantioenriched atropoisomeric 2-aryl-substituted 1,3-dienes, which have seldom been examined in previous literature. Catalytically relevant alkenyl palladacycles were synthesized and characterized by X-ray crystallography, and the energy profiles of the C(alkenyl)–H activation step and the stereoinduction model were elucidated by density functional theory (DFT) calculations.

Introduction

Alkenes react in a myriad of organometallic processes,[1] including nucleometallation,[2] migratory insertion,[3] C–H activation,[4] and isomerization.[5] Controlling selectivity among these pathways is critical for developing synthetically useful alkene functionalization methods. During the past few years, substrate-directed alkene functionalization has emerged as an enabling approach, in which selectivity control arises from coordination of the metal catalyst to Lewis basic sites on the substrate and subsequent formation of metalacyclic intermediates.[6]

We recently described methods for enantioselective hydroarylation and 1,2-arylfluorination of alkenyl aldehydes using a transient directing group (TDG)[7,8] strategy. In these systems an amino acid or amino amide co-catalyst reversibly condenses[9] with the alkenyl aldehyde substrate to generate an imine intermediate that is capable of coordinating to the palladium catalyst and directing arylpalladium(II) migratory insertion and downstream elementary steps. This TDG approach overcomes limitations associated with auxiliary-based methods,[10] which are widely used but add steps for auxiliary installation and cleavage. Based on these precedents, we questioned whether it would be possible to perturb this TDG-mediated alkene addition process such that C(alkenyl)–H activation[1b,4a,b,11] would occur in preference to migratory insertion (or nucleometallation) from a common π-alkene-palladium(II) complex. This would generate an *exo* alkenyl palladacycle capable of engaging in catalytic coupling with a potentially wide arsenal of reaction partners, thereby complementing other advances in TDG-based C–H functionalization,[12] which have largely focused on C(alkyl)–H,[13] C(benzyl)–H,[14] and C(aryl)–H,[15] substrates (Scheme 1A).[16,17] Herein, we describe the development of a TDG approach to C(alkenyl)–H alkenylation in which two C(alkenyl)–H bonds are oxidatively cross-coupled to generate 1,3-diene products.

[*] M. Liu, J. Sun, H.-Q. Ni, R. Martín-Montero, Prof. K. M. Engle
Department of Chemistry, The Scripps Research Institute
10550 N. Torrey Pines Road, La Jolla, CA 92037 (USA)
E-mail: keary@scripps.edu
T. G. Erbay, Prof. P. Liu
Department of Chemistry, University of Pittsburgh
Pittsburgh, PA 15260 (USA)
E-mail: pengliu@pitt.edu

[**] A previous version of this manuscript has been deposited on a preprint server (https://doi.org/10.26434/chemrxiv-2022-d0zfn).

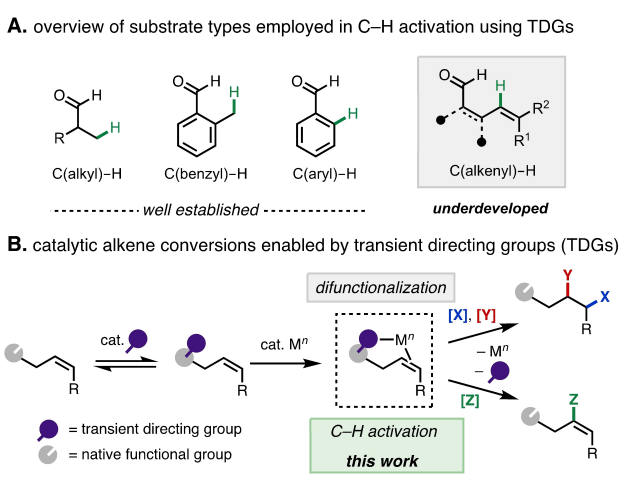

Scheme 1. Synopsis of prior work and current study.

Results and Discussion

To reduce this idea to practice, we carried out optimization with alkenyl aldehyde substrate **S1** and *tert*-butyl acrylate as the acceptor alkene. Using a previously published method as the starting point,[11d] we quickly recognized that the most important aspect of reaction optimization was identifying the optimal combination of TDG and carboxylate base to promote C(alkenyl)–H activation via a concerted metalation/deprotonation (CMD) process.[18,19] Screening of carboxylic acid additives as CMD bases (see Supporting Information) revealed that fluorine-containing benzoic acids are particularly effective in promoting the transformation.[14b] In particular, $\mathbf{A_{10}}$ emerged as the optimal additive, presumably due to having three electron-withdrawing groups without steric bulk at the 2 or 6 positions (see below). Having identified a suitable carboxylic acid additive, screening of α-amino acid TDGs[7,14a] showed the importance of the steric properties of the α-substituent. TDGs containing a branched α-substituent were more effective (Table 1), among which *tert*-leucine ($\mathbf{TDG_6}$) was the highest-yielding. In comparison, α,α-disubstituted amino acid $\mathbf{TDG_7}$ was much less effective, potentially due to being prohibitively rigid for the torsions required in the C-(alkenyl)–H activation step (see below).

With an efficient method in hand, we evaluated the substrate scope (Table 2). First, different substituents on the aromatic ring of the benzaldehyde moiety were examined. Electron-donating and electron-withdrawing groups were tolerated, providing good to high yields (**3**–**8**). In general electron-poor alkenyl benzaldehyde substrates were lower-yielding, as exemplified by product **2** containing a *para*-CF_3 group. Then, we tested substrates containing different substituents attached to the alkene (**9**–**14**). Beyond stilbene derivatives, *Z*-configured alkyl-substituted alkenes were also compatible. Whereas methyl-substituted substrate **9** gave only 32 % yield, branched alkyl groups were generally high-yielding (**10**–**13**). Analogous *E*-configured alkenes were ineffective substrates, leading to decomposition and unreacted starting material (see Supporting Information). Sterically hindered tri-substituted alkenes, which are a challenging class of substrates in C(alkenyl)–H activation,[1b,4a,b] were competent substrates in the case of benzylidenecyclobutane (**14**) and benzylidenepiperidine (**15**), furnishing highly substituted 1,3-diene products that would be otherwise difficult to prepare.

Table 1: Optimization of conditions.[a]

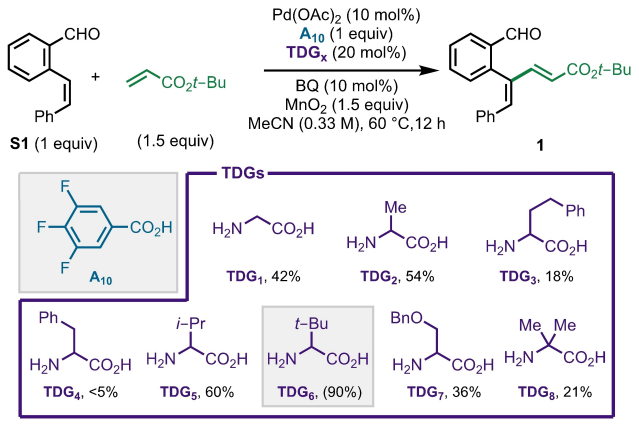

[a] Percentages represent ^{1}H-NMR yields with 1,3,5-trimethoxybenzene as internal standard; the value in parentheses represents isolated yield.

Table 2: Substrate scope.[a]

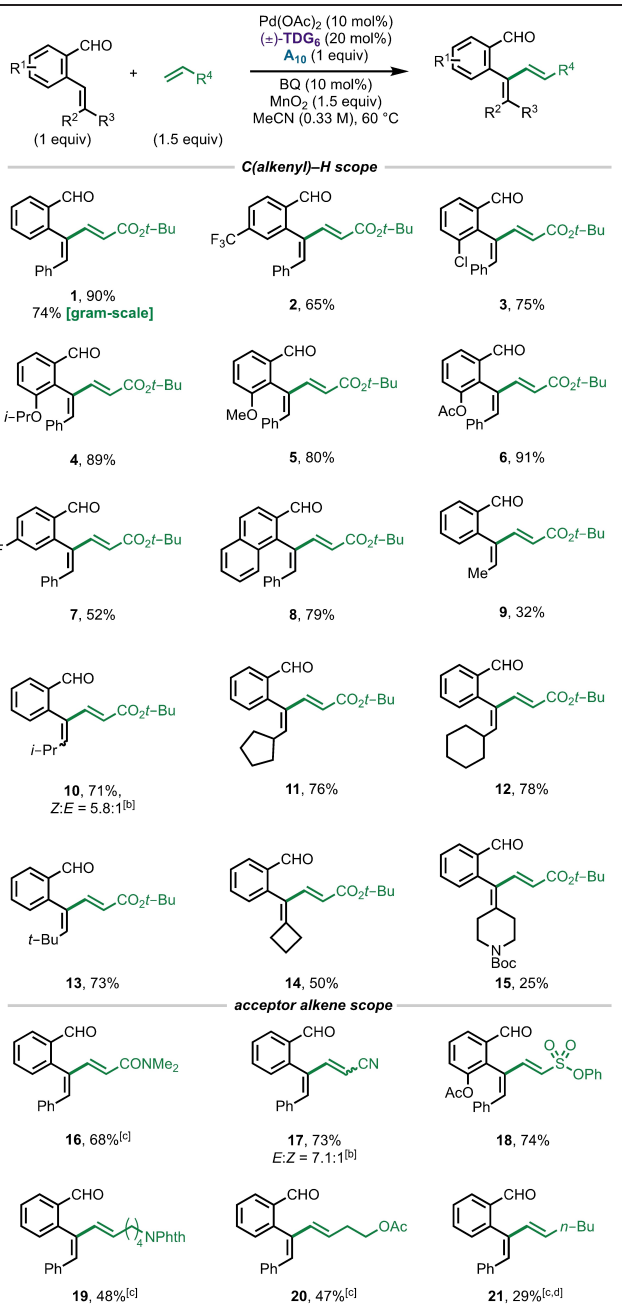

[a] Percentages represent isolated yields; (*Z*)-configured 1,2-disubstituted alkene starting materials were used in all cases. [b] Combined yield of *E* and *Z* isomers, which were separable. [c] 80 °C. [d] 20 mol % $Pd(OAc)_2$, 40 mol % $\mathbf{TDG_6}$.

In terms of the coupling partner scope, in addition to *tert*-butyl acrylate, other conjugated alkenes including *N*,*N*-dimethylacrylamide (**16**), acrylonitrile (**17**), and phenyl vinyl sulfonate (**18**) were effective. Moreover, non-conjugated alkenes were also viable coupling partners (**19**–**21**), though yields in these cases were lower. This reaction system is distinct compared to many previous Pd-catalyzed C–H alkenylation reactions because it successfully incorporates unreactive 1-hexene (**21**).[20,21] The method was demonstrated in a gram-scale reaction to prepare **1**, which proceeded in 74 % yield.

In preliminary experiments, we have found that this TDG-mediated C(alkenyl)–H activation method can be extended to a non-aromatic aldehyde substrate, namely (*Z*)-5-phenylpent-4-enal, albeit in low yield (Scheme 2). Compared to the standard conditions in Table 2, screening a small panel of conditions revealed that the 1,3-diene was produced by using PivOH as CMD promoter and conformationally constrained cyclopropane-based **TDG$_9$** as the TDG. Improved performance was achieved with a higher loading of the Pd catalyst and the TDG.

To demonstrate the utility of this C(alkenyl)–H alkenylation method, a representative product (**1**) was converted into a variety of useful derivatives (Figure 1). We were able to selectively reduce or oxidize the aldehyde moiety to prepare benzyl alcohol (**23**) and benzoic acid (**24**), respectively. Reductive decarboxylation could then be carried out from the benzoic acid to yield **25**,[22] allowing the aldehyde to function as a traceless directing group. Straightforward deprotection of the *t*-Bu ester with TFA yielded free dienyl acid **26**. Alternatively, both the aldehyde and the diene moieties could be simultaneously engaged in various annulation reactions. 3,4-Dihydroisoquinoline nitrone analogue **27** was prepared by treatment of **1** with hydroxylamine, which triggered condensation followed by aza-Michael addition.[23] Tetralone analogue **28** was obtained by Rh-catalyzed C(formyl)–H activation.[24]

With 3-substituted dienyl benzaldehyde products from Table 2, rotation about the C(aryl)–C(dienyl) bond was found to be restricted at ambient temperature. We thus questioned whether an enantioenriched TDG could be used to develop an atroposelective version of this transformation (Figure 2).[15d, 25–33] In comparison to axially chiral styrenes, synthesis of atropoisomeric 1,3-dienes are less explored owing to synthetic difficulties and facile product racemization (Figure 2A).[34–37] In one study, a C_2-symmetric cyclic 1,3-diene with large alkenyl substituents possessing a chiral axis along the C(alkenyl)–C(alkenyl) bond was synthesized, and the two atropoisomers were separated through chiral resolution.[37] Recently Shi reported the synthesis of enantioenriched 1,3-dienes containing a chiral C(aryl)–C(dienyl) axis via thioether-directed Pd^{II}-catalyzed C(alkenyl)–H activation to form an *endo*-palladacycle intermediate with a spirocyclic phosphoric acid as the chiral ligand.[38] Given that our approach proceeds via an *exo*-palladacycle, we imagined that it could offer access to a complementary collection of axially chiral 1,3-diene products. Thus, we optimized reaction conditions with respect to yield and *ee* for 3-substituted-2-alkenyl benzaldehyde substrates. We found that using L-*tert*-leucine (L-**TDG$_6$**) as TDG and carrying out the reaction at room temperature for four days afforded 1,3-dienes (**3**, **4**,

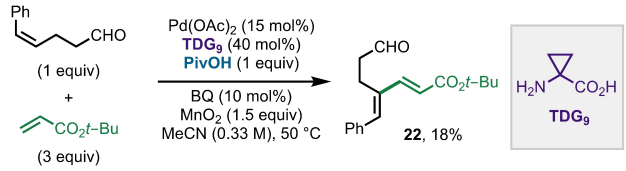

Scheme 2. Preliminary results with an aliphatic alkenyl aldehyde substrate.

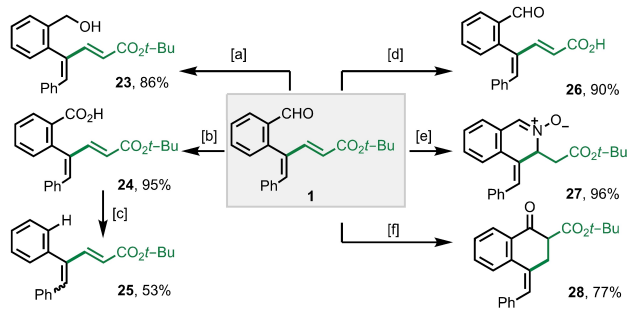

Figure 1. Product transformations. [a] $NaBH_4$ (1.5 equiv), MeOH, 0 °C–r.t., 2 h. [b] KH_2PO_4 (2.0 equiv), H_2O_2 (1.5 equiv), MeCN:H_2O = 2:1, then aq. $NaClO_2$ (1.5 equiv), 0 °C–r.t., 2 h. [c] $Pd(OAc)_2$ (5 mol %), dppb (10 mol %), Et_3SiH (1.5 equiv), Piv_2O (1.5 equiv), toluene, 160 °C, Ar, 9 h; the reaction generated a 2.4:1 mixture of *Z*/*E* isomers, which were separable; percentage value represents combined yield. [d] TFA (1.9 equiv), DCM, 0 °C–r.t., 30 min. [e] $NH_2OH{\cdot}HCl$ (1.2 equiv), Et_3N (1.3 equiv), THF, r.t., 14 h. [f] $[Rh(COD)Cl]_2$ (2.5 mol %), *rac*-BINAP (5 mol %), $NaBAr^F_4$ (5 mol %), 1,4-dioxane, 100 °C, Ar, 12 h.

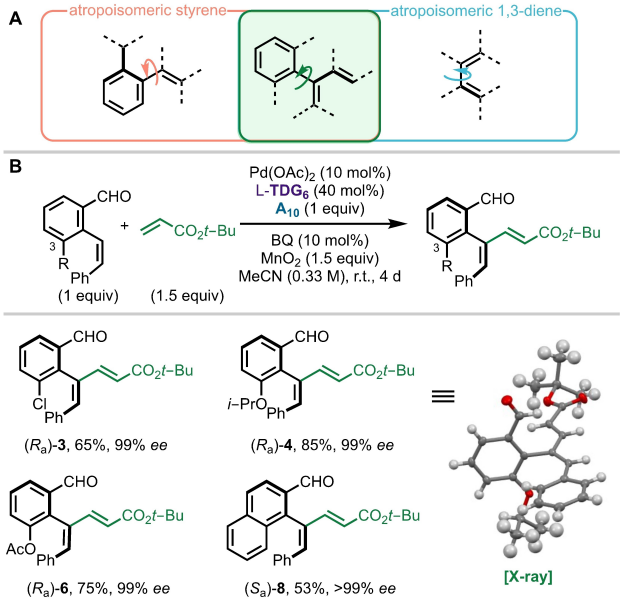

Figure 2. Syntheses of atropoisomeric 1,3-dienes. Left percentages represent isolated yields; absolute stereochemistry assigned in analogy to (R_a)-**4**.

6, and **7**) with good yield and excellent atroposelectivity (Figure 2B). X-ray crystallography was used to establish the absolute stereochemistry of the major isomer of **4** as R_a.

The high selectivity and critical role of the TDG and carboxylic acid promoter prompted us to examine the reaction mechanism through experimentation and theory. First, control experiments showed that these reaction conditions developed for C(alkenyl)–H activation were ineffective for analogous substrates bearing similarly positioned C(alkyl)–H and C(aryl)–H bonds (see Supporting Information), demonstrating the unique aspects of C-(alkenyl)–H activation in terms of electronic properties and transition state geometry. Next, by combining substrate **S1**, $Pd(OAc)_2$, and a TDG in pyridine,[13a, 39] we were able to prepare two alkenyl palladacycles, **29** and **30** (Figure 3). These complexes were obtained as a mixture of *E*/*Z*-stereoisomers,[5] with the product ratio influenced by the nature of the TDG. Complex **29** was further characterized by single-crystal X-ray diffraction confirming the *Z*-stereochemistry of the major isomer (aryl and Pd *cis* to each other). More facile *E*/*Z*-isomerization in this stoichiometric experiment with glycine (**TDG_1**, as in **29**) compared with *tert*-leucine (**TDG_6**, as in **30**) may explain the former's comparatively poor reactivity under catalytic conditions (Table 1). Notably, complex **29** is monomeric in contrast to the dimeric *exo*-alkenyl palladacycle complex previously obtained in our investigations of 8-aminoquinoline-amide-directed C(alkenyl)–H activation.[11d] Complex **30** was found to be catalytically competent, despite containing a pyridine ligand that is not present under catalytic conditions (see Supporting Information).

A plausible catalytic cycle (Scheme 3) is proposed based on the experimental mechanistic studies and prior work.[7,8,11d] Following coordination with the condensed imine, a π-alkene complex is formed, and the carboxylate-assisted C–H metalation occurs via a concerted metalation-deprotonation (CMD) mechanism to generate a six-membered palladacycle. Ligand exchange with the alkene is followed by migratory insertion to form an eight-membered palladacycle. The diene product is then formed via β-hydride elimination and directing group dissociation. Oxidation of the Pd^0 species and coordination of another condensed imine substrate regenerate the catalyst/reactant complex.

We performed density functional theory (DFT) calculations to investigate the proposed mechanism and the origin of the atroposelectivity (Figure 4).[40] The reaction free energy profile of the C–H alkenylation of alkenyl aldehyde **S1** with *tert*-butyl acrylate using L-*tert*-leucine (L-**TDG_6**) as

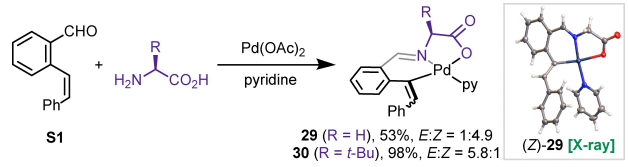

Figure 3. Synthesis of alkenyl palladacycle complexes. The stereochemistry of (*E*)-**30** and (*Z*)-**30** was assigned in by ^{1}H-NMR in analogy to (*E*)-**29** and (*Z*)-**29**.

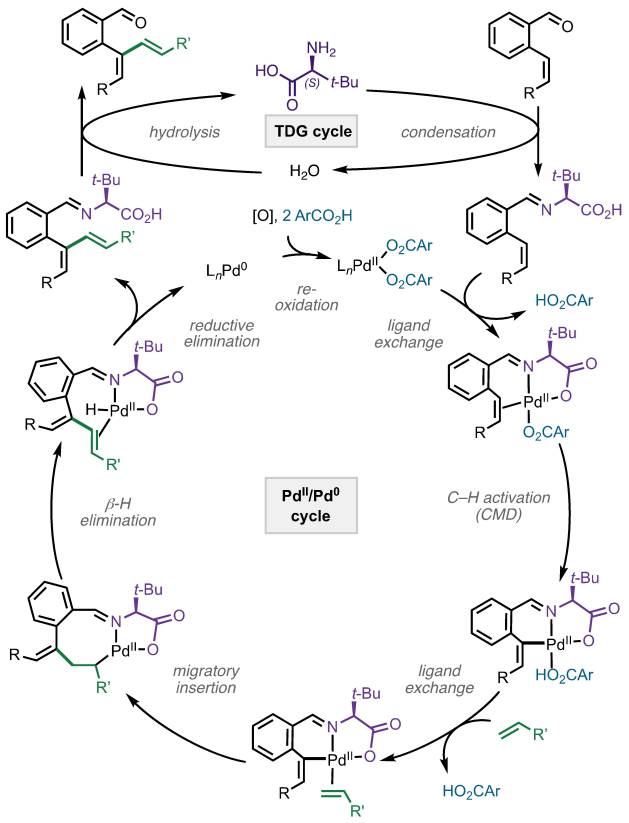

Scheme 3. Proposed catalytic cycle.

the TDG and 3,4,5-trifluorobenzoic acid (**A_{10}**) additive was computed at the M06/6-311 + G(d,p)-SDD(Pd)/SMD-(MeCN)//M06/6-31G(d)-SDD(Pd) level of theory (Figure 4A).[41] From the most stable isomer of the *N*-,*O*-coordinated π-alkene complex **IM1**, the carboxylate-assisted alkenyl C–H metalation occurs via a CMD mechanism via transition state **TS1**.[42] The resulting six-membered palladacycle **IM3** undergoes ligand exchange to replace the coordinated benzoic acid with *tert*-butyl acrylate to form more stable intermediates **IM4a** and **IM4b**, where two opposite π-faces of the *tert*-butyl acrylate bind to the Pd center. Alkene migratory insertion from **IM4a** and **IM4b** (via **TS3a** and **TS3b**) leads to eight-membered palladacycles **IM5a** and **IM5b** that are both stabilized by coordination of the π bond on the γ carbon to the Pd center. A relatively small (1.5 kcal mol^{-1}) energy difference between **TS3a** and **TS3b** is observed—here, **TS3a** is slightly more stable due to less steric repulsion between the *tert*-butyl acrylate and the carboxylate oxygen on the TDG (see Supporting Information for 3D structures of **TS3a** and **TS3b**). Upon β-hydride elimination and directing group dissociation, **IM5a** and **IM5b** form the same 1,3-diene product.

Next, we investigated the origin of atroposelectivity in the C–H alkenylation. Because the C–H metalation step is computationally determined to be irreversible and the rotation about the C(aryl)–C(alkenyl) bond is hindered after palladacycle formation, the atroposelectivity of the 1,3-diene product is determined in the C–H metalation step. We

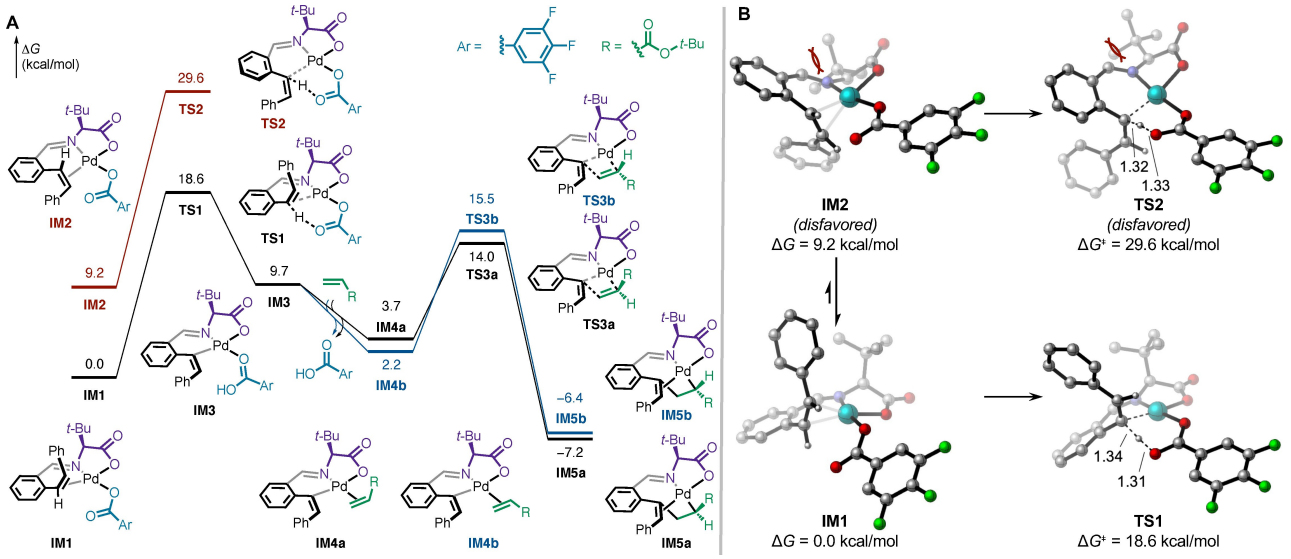

Figure 4. Computational studies. A) Calculated reaction energy profile of C–H alkenylation of alkenyl aldehyde **S1** with *L-tert*-leucine as TDG. B) Origin of atroposelectivity.

computed the C(alkenyl)–H metalation pathways from two π-alkene complexes (**IM1** and **IM2**, Figure 4B), where two different π-faces of the alkene bind to the Pd center, leading to two atropoisomers. The chiral center on the TDG significantly impacts the relative stabilities of these two π-alkene complexes and subsequent C–H metalation transition states (**TS1** and **TS2**). In the less stable π-alkene complex **IM2**, the Pd center is significantly distorted from square planar geometry, making it 9.2 kcal mol^{-1} higher in energy than **IM1** (Figure 4B). Similar distortion is observed in **TS2**, which is 11.0 kcal mol^{-1} higher in energy than **TS1**. The distortion in **IM2** and **TS2** is caused by steric repulsion between the *t*-Bu group on the TDG and the imine carbon, which are *syn*-periplanar in **IM2** and **TS2**. Such steric repulsion is diminished in **IM1** and **TS1**, where the Ph group on the imine is not co-planar with the *t*-Bu. Although the atroposelectivity of the 1,3-diene product **1** is ablated due to the lack of *ortho*-substituent on the Ar group allowing free rotation about the C(aryl)–C(dienyl) bond, the predicted atroposelectivity is consistent with the X-ray crystal structure of the *o*-O*i*-Pr substituted product **4**.

Conclusion

In summary, we have developed a TDG-enabled, Pd^{II}-catalyzed C(alkenyl)–H alkenylation, affording 1,3-dienes with excellent regio- and *E*/*Z*-selectivity. We demonstrated the utility of this method through various product derivatizations and applied an atroposelective version of the transformation to synthesize a rare class of enantioenriched axially chiral 1,3-dienes. Key aspects of the reaction mechanism were elucidated through the synthesis of two alkenyl palladacycle complexes and computational studies of key steps in the catalytic cycle. This study establishes a foundation for future work on TDG-mediated, Pd-catalyzed alkene functionalization and advances the state of the art in C(alkenyl)–H activation methodology.

Acknowledgements

This work was financially supported by the National Science Foundation (CHE-2046286 and CHE-1654122) and the Research Corporation for Science Advancement (Cottrell Scholars Program). R.M.-M. was supported by a La Caixa Predoctoral Fellowship. We thank Quynh Nguyen Wong, Emily J. Sturgell, Brittany B. Sanchez, and Dr. Jason S. Chen (Scripps Research Automated Synthesis Facility) for HRMS analysis, SFC separation of atropoisomers, and compound purification. We also thank Dr. Milan Gembicky (UCSD) for X-ray crystallography analysis and Prof. De-Wei Gao (ShanghaiTech) for helpful discussions. DFT calculations were carried out at the Center for Research Computing at the University of Pittsburgh and the Extreme Science and Engineering Discovery Environment (XSEDE).

Conflict of Interest

The authors declare no conflict of interest.

Data Availability Statement

The data that support the findings of this study are openly available in CCDC 2023071.

Keywords: 1,3-Dienes · Atropisomers · C–H Activation · Palladium · Transient Directing Group

[1] a) R. H. Crabtree, *The Organometallic Chemistry of the Transition Metals*, 6th ed., Wiley, Hoboken, **2014**, pp. 224–258; b) M. Liu, J. Sun, K. M. Engle, *Tetrahedron* **2022**, *103*, 132513.

[2] For reviews, see: a) R. I. McDonald, G. Liu, S. S. Stahl, *Chem. Rev.* **2011**, *111*, 2981–3019; b) P. Kočovský, J.-E. Bäckvall, *Chem. Eur. J.* **2015**, *21*, 36–56.

[3] For reviews, see: a) R. F. Heck, *Acc. Chem. Res.* **1979**, *12*, 146–151; b) I. P. Beletskaya, A. V. Cheprakov, *Chem. Rev.* **2000**, *100*, 3009–3066; c) A. B. Dounay, L. E. Overman, *Chem. Rev.* **2003**, *103*, 2945–2964; d) R. J. DeLuca, B. J. Stokes, M. S. Sigman, *Pure Appl. Chem.* **2014**, *86*, 395–408.

[4] For reviews of C(alkenyl)–H activation, see: a) X. Shang, Z.-Q. Liu, *Chem. Soc. Rev.* **2013**, *42*, 3253–3260; b) B. Liu, L. Yang, P. Li, F. Wang, X. Li, *Org. Chem. Front.* **2021**, *8*, 1085–1101; for representative reports on C(allylic)–H activation, see: c) M. S. Chen, N. Prabagaran, N. A. Labenz, M. C. White, *J. Am. Chem. Soc.* **2005**, *127*, 6970–6971; d) L.-F. Fan, P.-S. Wang, L.-Z. Gong, *Org. Lett.* **2019**, *21*, 6720–6725.

[5] For representative reports, see: a) J. Yu, M. J. Gaunt, J. B. Spencer, *J. Org. Chem.* **2002**, *67*, 4627–4629; b) E. H. P. Tan, G. C. Lloyd-Jones, J. N. Harvey, A. J. J. Lennox, B. M. Mills, *Angew. Chem. Int. Ed.* **2011**, *50*, 9602–9606; *Angew. Chem.* **2011**, *123*, 9776–9780; c) R. Matsuura, M. K. Karunananda, M. Liu, N. Nguyen, D. G. Blackmond, K. M. Engle, *ACS Catal.* **2021**, *11*, 4239–4246.

[6] For reviews, see: a) A. H. Hoveyda, D. A. Evans, G. C. Fu, *Chem. Rev.* **1993**, *93*, 1307–1370; b) M. Oestreich, *Eur. J. Org. Chem.* **2005**, 783–792; c) M. Oestreich, *Top. Organomet. Chem.* **2007**, *24*, 169–192; d) G. Rousseau, B. Breit, *Angew. Chem. Int. Ed.* **2011**, *50*, 2450–2494; *Angew. Chem.* **2011**, *123*, 2498–2543.

[7] L. J. Oxtoby, Z.-Q. Li, V. T. Tran, T. G. Erbay, R. Deng, P. Liu, K. M. Engle, *Angew. Chem. Int. Ed.* **2020**, *59*, 8885–8890; *Angew. Chem.* **2020**, *132*, 8970–8975.

[8] Z. Liu, L. J. Oxtoby, M. Liu, Z.-Q. Li, V. T. Tran, Y. Gao, K. M. Engle, *J. Am. Chem. Soc.* **2021**, *143*, 8962–8969.

[9] C.-H. Jun, H. Lee, J.-B. Hong, *J. Org. Chem.* **1997**, *62*, 1200–1201.

[10] For reviews, see: a) J. Derosa, V. T. Tran, V. A. van der Puyl, K. M. Engle, *Aldrichimica Acta* **2018**, *51*, 21–32; b) C. Lin, L. Shen, *ChemCatChem* **2019**, *11*, 961–968; c) L. M. Wickham, R. Giri, *Acc. Chem. Res.* **2021**, *54*, 3415–3437.

[11] For representative reports, see: a) Y.-H. Xu, J. Lu, T.-P. Loh, *J. Am. Chem. Soc.* **2009**, *131*, 1372–1373; b) H. Zhou, Y.-H. Xu, W.-J. Chung, T.-P. Loh, *Angew. Chem. Int. Ed.* **2009**, *48*, 5355–5357; *Angew. Chem.* **2009**, *121*, 5459–5461; c) Q.-J. Liang, C. Yang, F.-F. Meng, B. Jiang, Y.-H. Xu, T.-P. Loh, *Angew. Chem. Int. Ed.* **2017**, *56*, 5091–5095; *Angew. Chem.* **2017**, *129*, 5173–5177; d) M. Liu, P. Yang, M. K. Karunananda, Y. Wang, P. Liu, K. M. Engle, *J. Am. Chem. Soc.* **2018**, *140*, 5805–5813; e) B. S. Schreib, E. M. Carreira, *J. Am. Chem. Soc.* **2019**, *141*, 8758–8763; f) K. Meng, T. Li, C. Yu, C. Shen, J. Zhang, G. Zhong, *Nat. Commun.* **2019**, *10*, 5109; g) Y.-C. Luo, C. Yang, S.-Q. Qiu, Q.-J. Liang, Y.-H. Xu, T.-P. Loh, *ACS Catal.* **2019**, *9*, 4271–4276; h) B. S. Schreib, M. Fadel, E. M. Carreira, *Angew. Chem. Int. Ed.* **2020**, *59*, 7818–7822; *Angew. Chem.* **2020**, *132*, 7892–7896; i) Z. Wu, N. Fatuzzo, G. Dong, *J. Am. Chem. Soc.* **2020**, *142*, 2715–2720; j) C. Shen, Y. Zhu, S. Jin, K. Xu, S. Luo, L. Xu, G. Zhong, L. Zhong, J. Zhang,, *Org. Chem. Front.* **2022**, *9*, 989–994.

[12] For reviews, see: a) C.-H. Jun, C. W. Moon, D.-Y. Lee, *Chem. Eur. J.* **2002**, *8*, 2422–2428; b) D. A. Colby, R. G. Bergman, J. A. Ellman, *Chem. Rev.* **2010**, *110*, 624–655; c) Q. Zhao, T. Poisson, X. Pannecoucke, T. Besset, *Synthesis* **2017**, *49*, 4808–4826; d) P. Gandeepan, L. Ackermann, *Chem* **2018**, *4*, 199–222; e) J. I. Higham, J. A. Bull, *Org. Biomol. Chem.* **2020**, *18*, 7291–7315; f) N. Goswami, T. Bhattacharya, D. Maiti, *Nat. Rev. Chem.* **2021**, *5*, 646–659.

[13] a) K. Yang, Q. Li, Y. Liu, G. Li, H. Ge, *J. Am. Chem. Soc.* **2016**, *138*, 12775–12778; b) Y. Wu, Y.-Q. Chen, T. Liu, M. D. Eastgate, J.-Q. Yu, *J. Am. Chem. Soc.* **2016**, *138*, 14554–14557; c) Y. Liu, H. Ge, *Nat. Chem.* **2017**, *9*, 26–32; d) Y.-Q. Chen, Y. Wu, Z. Wang, J. X. Qiao, J.-Q. Yu, *ACS Catal.* **2020**, *10*, 5657–5662; e) Y.-Q. Chen, S. Singh, Y. Wu, Z. Wang, W. Hao, P. Verma, J. X. Qiao, R. B. Sunoj, J.-Q. Yu, *J. Am. Chem. Soc.* **2020**, *142*, 9966–9974.

[14] a) F.-L. Zhang, K. Hong, T.-J. Li, H. Park, J.-Q. Yu, *Science* **2016**, *351*, 252–256; b) H. Park, P. Verma, K. Hong, J.-Q. Yu, *Nat. Chem.* **2018**, *10*, 755–762.

[15] a) R. B. Bedford, S. J. Coles, M. B. Hursthouse, M. E. Limmert, *Angew. Chem. Int. Ed.* **2003**, *42*, 112–114; *Angew. Chem.* **2003**, *115*, 116–118; b) X.-Y. Chen, E. J. Sorensen, *J. Am. Chem. Soc.* **2018**, *140*, 2789–2792; c) C. Yang, F. Li, T.-R. Wu, R. Cui, B.-B. Wu, R.-X. Jin, Y. Li, X.-S. Wang, *Org. Lett.* **2021**, *23*, 8132–8137; d) H. Song, Y. Li, Q.-J. Yao, L. Jin, L. Liu, Y.-H. Liu, B.-F. Shi, *Angew. Chem. Int. Ed.* **2020**, *59*, 6576–6580; *Angew. Chem.* **2020**, *132*, 6638–6642; e) J. Xu, Y. Liu, J. Zhang, X. Xu, Z. Jin, *Chem. Commun.* **2018**, *54*, 689–692.

[16] Dong has developed α-C(sp^3)–H functionalization reactions of ketones via C(alkenyl)–H activation of in situ generated or preformed enamines/enamides. For a review, see: a) H. N. Lim, D. Xing, G. Dong, *Synlett* **2019**, *30*, 674–684; for examples where the DG is used stoichiometrically, see: b) Z. Wang, B. J. Reinus, G. Dong, *J. Am. Chem. Soc.* **2012**, *134*, 13954–13957; c) Z. Wang, B. J. Reinus, G. Dong, *Chem. Commun.* **2014**, *50*, 5230–5232; d) D. Xing, G. Dong, *J. Am. Chem. Soc.* **2017**, *139*, 13664–13667; For examples where the DG is used catalytically (i.e., as a TDG), see: e) F. Mo, H. N. Lim, G. Dong, *J. Am. Chem. Soc.* **2015**, *137*, 15518–15527; f) F. Mo, G. Dong, *Science* **2014**, *345*, 68–72; g) D. Xing, X. Qi, D. Marchant, P. Liu, G. Dong, *Angew. Chem. Int. Ed.* **2019**, *58*, 4366–4370; *Angew. Chem.* **2019**, *131*, 4410–4414.

[17] For rare examples of TDG-enabled C(alkenyl)–H activation involving *endo* metallacycles that yield functionalized alkene products, see: a) C.-H. Jun, C. W. Moon, Y.-M. Kim, H. Lee, J. H. Lee, *Tetrahedron Lett.* **2002**, *43*, 4233–4236; b) X.-Y. Chen, E. J. Sorensen, *Chem. Sci.* **2018**, *9*, 8951–8956. In parallel to the current study, Zhong and Zhang reported a complementary Pd^{II}/TDG-mediated *endo*-selective C(alkenyl)–H alkenylation of 1,1-disubstituted alkenyl benzaldehyde substrates: c) C. Shen, Y. Zhu, W. Shen, S. Jin, G. Zhong, S. Luo, L. Xu, L. Zhong, J. Zhang, *Org. Chem. Front.* **2022**, *9*, 2109–2115.

[18] a) D. Lapointe, K. Fagnou, *Chem. Lett.* **2010**, *39*, 1118–1126; b) D. L. Davies, S. A. Macgregor, C. L. McMullin, *Chem. Rev.* **2017**, *117*, 8649–8709.

[19] a) D. L. Davies, S. M. A. Donald, S. A. Macgregor, *J. Am. Chem. Soc.* **2005**, *127*, 13754–13755; b) H.-Y. Sun, S. I. Gorelsky, D. R. Stuart, L.-C. Campeau, K. Fagnou, *J. Org. Chem.* **2010**, *75*, 8180–8189; c) L. Wang, B. P. Carrow, *ACS Catal.* **2019**, *9*, 6821–6836.

[20] K. M. Engle, D.-H. Wang, J.-Q. Yu, *J. Am. Chem. Soc.* **2010**, *132*, 14137–14151.

[21] A. Deb, A. Hazra, Q. Peng, R. S. Paton, D. Maiti, *J. Am. Chem. Soc.* **2017**, *139*, 763–775.

[22] C. Liu, Z.-X. Qin, C.-L. Ji, X. Hong, M. Szostak, *Chem. Sci.* **2019**, *10*, 5736–5742.

[23] L. R. Peacock, R. S. L. Chapman, A. C. Sedgwick, M. F. Mahon, D. Amans, S. D. Bull, *Org. Lett.* **2015**, *17*, 994–997.

[24] K. F. Johnson, A. C. Schmidt, L. M. Stanley, *Org. Lett.* **2015**, *17*, 4654–4657.

[25] Q.-J. Yao, S. Zhang, B.-B. Zhan, B.-F. Shi, *Angew. Chem. Int. Ed.* **2017**, *56*, 6617–6621; *Angew. Chem.* **2017**, *129*, 6717–6721.

[26] G. Liao, B. Li, H.-M. Chen, Q.-J. Yao, Y.-N. Xia, J. Luo, B.-F. Shi, *Angew. Chem. Int. Ed.* **2018**, *57*, 17151–17155; *Angew. Chem.* **2018**, *130*, 17397–17401.
[27] J. Luo, T. Zhang, L. Wang, G. Liao, Q.-J. Yao, Y.-J. Wu, B.-B. Zhan, Y. Lan, X.-F. Lin, B.-F. Shi, *Angew. Chem. Int. Ed.* **2019**, *58*, 6708–6712; *Angew. Chem.* **2019**, *131*, 6780–6784.
[28] G. Liao, H.-M. Chen, Y.-N. Xia, B. Li, Q.-J. Yao, B.-F. Shi, *Angew. Chem. Int. Ed.* **2019**, *58*, 11464–11468; *Angew. Chem.* **2019**, *131*, 11586–11590.
[29] L. Jin, Q.-J. Yao, P.-P. Xie, Y. Li, B.-B. Zhan, Y.-Q. Han, X. Hong, B.-F. Shi, *Chem* **2020**, *6*, 497–511.
[30] U. Dhawa, C. Tian, T. Wdowik, J. C. A. Oliveira, J. Hao, L. Ackermann, *Angew. Chem. Int. Ed.* **2020**, *59*, 13451–13457; *Angew. Chem.* **2020**, *132*, 13553–13559.
[31] C. Yang, T.-R. Wu, Y. Li, B.-B. Wu, R.-X. Jin, D.-D. Hu, Y.-B. Li, K.-J. Bian, X.-S. Wang, *Chem. Sci.* **2021**, *12*, 3726–3732.
[32] G. Liao, T. Zhou, Q.-J. Yao, B.-F. Shi, *Chem. Commun.* **2019**, *55*, 8514–8523.
[33] S. Zhang, G. Liao, B.-F. Shi, *Chin. J. Org. Chem.* **2019**, *39*, 1522–1528.
[34] M. Rösner, G. Köbrich, *Angew. Chem. Int. Ed. Engl.* **1974**, *13*, 741–742; *Angew. Chem.* **1974**, *86*, 775–776.
[35] S. Warren, A. Chow, G. Fraenkel, T. V. RajanBabu, *J. Am. Chem. Soc.* **2003**, *125*, 15402–15410.
[36] N. Shindoh, Y. Takemoto, K. Takasu, *Chem. Eur. J.* **2009**, *15*, 7026–7030.
[37] M. Ogasawara, S. Kotani, H. Nakajima, H. Furusho, M. Miyasaka, Y. Shimoda, W.-Y. Wu, M. Sugiura, T. Takahashi, M. Nakajima, *Angew. Chem. Int. Ed.* **2013**, *52*, 13798–13802; *Angew. Chem.* **2013**, *125*, 14043–14047.
[38] a) L. Jin, P. Zhang, Y. Li, X. Yu, B.-F. Shi, *J. Am. Chem. Soc.* **2021**, *143*, 12335–12344; while the current manuscript was under review, a related transformation was described: b) D.-T. Dai, M.-W. Yang, Z.-Y. Chen, Z.-L. Wang, Y.-H. Xu, *Org. Lett.* **2022**, *24*, 1979–1984.
[39] X.-Y. Chen, S. Ozturk, E. J. Sorensen, *Org. Lett.* **2017**, *19*, 1140–1143.
[40] For recent computational studies on atroposelective C–H functionalization using directing group strategies, see: a) Q.-J. Yao, P.-P. Xie, Y.-J. Wu, Y.-L. Feng, M.-Y. Teng, X. Hong, B.-F. Shi, *J. Am. Chem. Soc.* **2020**, *142*, 18266–18276; b) U. Dhawa, T. Wdowik, X. Hou, B. Yuan, J. C. A. Oliveira, L. Ackermann, *Chem. Sci.* **2021**, *12*, 14182–14188.
[41] a) Y. Zhao, D. G. Truhlar, *Theor. Chem. Acc.* **2008**, *120*, 215–241; b) A. V. Marenich, C. J. Cramer, D. G. Truhlar, *J. Phys. Chem. B* **2009**, *113*, 6378–6396.
[42] When 2,4,6-trifluorobenzoate is used as the base in the CMD transition state, the computed barrier for C–H metalation is 1.1 kcal mol^{-1} higher than **TS1**. This is consistent with the higher efficiency of $\mathbf{A_{10}}$ as the additive. See Figure S2 in the Supporting Information for details.

Manuscript received: March 10, 2022
Accepted manuscript online: April 25, 2022
Version of record online: May 26, 2022